Airborne Infrared Spectroscopy Of 1994 Western Wildfires

Helen Worden, Reinhard Beer
Jet Propulsion Laboratory
California Institute of Technology
PASADENA, CA 91109

Curtis J. Rinsland
NASA Langley Research Center
HAMPTON, VA 23665

ABSTRACT

In the summer of 1994, the 0.07 cm^{-1} resolution infrared Airborne Emission Spectrometer (AES) acquired spectral data over two wildfires, one in central Oregon on August 3 and the other near San Luis Obispo, California on August 15. The spectrometer was on board a NASA DC-8 research aircraft, flying at an altitude of 12, km. The spectra from both fires clearly show features due to water vapor, carbon dioxide, carbon monoxide, ammonia, methanol, formic acid and ethylene at significantly higher abundance and temperature than observed in downlooking spectra of normal atmospheric and ground conditions. Column densities are derived for several species at 11. Molar ratios are compared with previous biomass fire measurements. We believe that this is the first time such data have been acquired by airborne spectral remote sensing.

introduction

During late July and early August 1994, hot, dry weather and abundant overgrowth precipitated several wildfires in the Pacific Northwest and California. On the afternoon of August 3, the NASA DC-8 research aircraft was returning to its base at Moffett Field, CA from a flight planned for Synthetic Aperture Radar (SAR) measurements when the flight line was re-directed to make an overpass of one of these fires (some 65 km east of Mt. Hood at latitude 45°19' N; longitude 120° 52' W). Accompanying the SAR was the new 0.07 cm^{-1} resolution infrared Airborne Emission Spectrometer (AES) which succeeded in obtaining a series of spectra (in the 4.5 to 13.5 μ range) beginning at 22:58:24 UT. The AES field of view was locked onto flames of the fire by an interactive video tracker for the 30 seconds that the fire was visible through the viewpoint installed in the cargo hold of the aircraft. Strong emission lines of water vapor (H_2O), carbon dioxide (CO_2) and carbon monoxide (CO) emanating from highly excited states, indicative of a gas cloud at elevated temperatures, were clearly visible in a preliminary examination of the spectral data. Absorption features due to ammonia (NH_3) were also obvious.

A second series of wildfire spectra was taken on August 15, 1994 in California with the AES on board the same aircraft at 35° 14' N, 120° 41' W, about 10 km north-west of San Luis Obispo, CA. This second set of spectra was also obtained as a target of opportunity on a flight with a different primary mission plan, however, more time was available for three overpasses of the fire line and a total of 90 seconds of spectral data was collected

direct] y over flaming areas, as wel 1 as data from near by unburned areas. A quick inspection of the spect ra from the Californiafire revealed, as in the data from the Oregon fire, strong H_2O, CO_2 and CO emission lines as well as higher levels of saturation in the N] I_3 and CO absorption features than observed for the Oregon fire.

Since these observations were not 1):)11 of a planned experiment, there was no other instrumentation to provide in-situ measurements as input or verificat ion for a model of the ground and atmospheric state parameters. Nonetheless, we have developed a provisional physical model of the observed fire scene to match our spectra l observations. Using this model, and relying on relative spectral features as much as possible, wc. have. been able to quantify the flame temperatures, and the C"O, NH_3, (.31~011 and 1 ICOOI I column densities. Since H_2O and CO_2 have a large background abundance, the fit to the spectral features is too model dependent to give, reliable est imate of the.ir excess abundance from the fires.

1 missions from biomass burning ar c widely recognized as a significant source of pollution affecting atmospheric chemistry, photochemistry and trace gas concentrat ions [cf. *Crutzen and Andreae,* 1990]. The spectral IGI note sensing technique holds many advantages for measuring emissions from biomass fires In general, detectable quantities of gases are higher than those for *in situ* sampling, however, many species are above these detection limits in forest fire observations. 1)ue to the difficulties in sample collection, there are few *in situ* measurements of emission factors for reactive species such as methanol and formic acid while a spectrometer can track the abundance of these species in all phases of a fire [*Griffith, et al.*, 1991; *Yokelson, et al.*, 1995]. Species can be measured simultaneously with none of the uncertainties inherent to the separate handling procedures of *in situ* measurements. Ammonia, which has an especially distinct IR spectral signature, can be measured with good precision in contrast to errors as large as 50% for *in situ* sampling of NH_3 in smoke plumes [*Laursen et al.*, 1992]. 1 lame temperatures can be estimated and could be useful to other remotely sensed radiometry measurements. Some important species, such as NO and NO_2, are difficult to measure with nadir viewing space or airborne spectral remote sensing due to obscuration by atmospheric water vapor absorption, alt bough these species at e easi I y measured in ground based spectral remote sensing [*Griffith, et al.*, 1991; *Yokelson, et al.*, 1995]. Other commonly emitted species such as methane and formaldehyde have 1 R spectral signatures that are not obscured in the nadir view through the atmosphere and were simply outside the frequency ranges in these data.

Fire 1)escriptions

The August 3, 1994 fire observed tit, 45" i 9' h'. 120° 52' W, near the Deshutes river, was one of the many relatively small fires i n the area just east of the Cascades range in Washington and Oregon on that day. The best estimate from the Bureau of 1 .and Management [*BLM,* 1995] was that the fire was on private land with mostl y grass, shrubs and sage brush on slopes and a few alder and juniper trees in the lower canyon areas.

The August 1 S, 1995 observation al 35° 2/1' N 1 20° 41' w was of a large brush fire, designated the. 1 lighway 41 fire., that sta I ted on August 14, 1994 and moved south-cast

toward San Luis Obispo, CA. This fire was considered the largest California wildfire of 1994, with a total of 45400 acres burned '1 t ie I orest Service [*Cal. Dept. Forestry,* 1995] described this fire as a type. 4 heavy brusl 1 icad fire and estimated a fuel load of 20 to 25 tons/acre. A survey of vegetation coverage for the private and public lands burred gave 60% brush (chemise, manzanita), 30% oak woodland, 1 ()% grassland and 1 % conifer.

The AES instrument and Observational Approach

AES is a Fourier Transform spectrometer (t TS) specifically designed to acquire line wiclth-limited (<0.1 cm-1) infrared spectra of the 10 WC] atmosphere through a ZnSe window in the underside of an aircraft. Radiation traversing the window is intercepted by a TV-guided 2-axis pointing system. When observing localized targets over land, the pointing system can either be locked onto the source 01 set into an open-loop rate compensation mode. (In the collection of data over burning areas, the flames provided sufficient visible contrast to acquire a target lock.) The locked and rate compensation modes allow data sets to be acquired over about 30 seconds (limited by the size of the window) before the system is rc.set to its forward position. Alternatively, the pointing system can simply be set into a nadir staring mode, in which case. data acquisition is continuous. in any event, the view seen by the t racking camera is recorded on a conventional VCR that is time-tap,p,cd identical I y to the infrared data 'l'he. same pointing mirror is also used to make frequent (every 3(I minutes or less) observations of on-board black-body radiometric calibration sources (essential for the retrieval process).

Fig. 1 shows optical schematics of the interferometer and the periscope and tracking system. The infrared beam passes via the periscope into the interferometer that is the heart of the 1 '1'S. The interferometer consists of a beamsplitter/recombiner of Ge-coated KBr that divides the beam into two (nominally 50-50), one of which travels to a fixed cube-corner reflector (CCR) and the other to another CCR that move.s on a carriage driven by a leadscrew/DC motor combination, thereby imposing an optical path difference between the two arms. Frequency (wavelength) calibration of an FTS is unnecessary since the optical path difference is continuously measured by an internal Nd:YAG laser traversing the same optical system as the infrared beam.

Data are acquired with the moving ('(CR traveling in both directions (2 seconds end-to-end). About 1 second is required to reverse directions. The motion of the CCR impresses an amplitude modulation on the infrared beam that is subsequently sensed and recorded by 4 sets of 1 IgCdTe infrared detectors (eac I opt i mized for a different spectral region). Each individual detector set (maintain ed at 65 K by) romping on 1 .N2 dewars) has 4 adjacent pixels (optically- conjugated dewar-to-dewar) Thus 16 interferograms (and therefore spectra) arc recorded in parallel on 8mm d i gite 1 t ape (together with pertinent engineering and navigation data) after being digitized with 16-bit A-D converters. Within each dewar arc sets of interchangeable ("on the fly") band pass filters about 200 cm^{-1} wide whose primary function is to limit the ambient-temperature thermal background from compromising signal-to-noise ratio. Subsequent data processing is performed off- line. This processing includes converting the interferograms to spectra, phase correcting the spectra, converting the calibration spectra to gain and offset functions and applying the gain and OffSCt to the target spectra.

AES Fire Data

Figures 2 and 3 show the AI ES spectra taken from the Oregon (OR) and California (CA) fires as well as spectra taken from an unburned area upwind of the California fire. The spectral bands shown are 950 to 1150 cm^{-1} (8.7 to 10.5 μ) and 1960 102060 cm^{-1} (4.9 to *5.1 p).* These bands show many of the interesting spectral features due to the fire and the figures represent most of the data used in this analysis. Unfortunately, WC. could not use the data in the 1200 to 1400 cm^{-1} (7, I to 8.3 μ) spectral region due to problems with one of the dewars. Normally, this is the region where we obtain spectral information for methane, a common emission in biomass fires.

The signals for the spectra shown in 1 ig 2 were converted to radiance units using calibration data from the onboard blackbody at temperatures 290 K and 350 K. These calibration data give a gain and offset value at each sampled frequency. The gain has units of data number (DN) per unit radiance (Watts/cm^2/sr/cm^{-1}). The offset, which is subtracted from target spectra, is due to the f I ux contribution from the instrument at ambient aircraft temperature. I 'or most observations, these blackbody temperatures span the range of ground target temperatures. but for the. forest fires, this was not the case, Since wc did not have a higher temperature calibration point available, wc must assume the gain has a linear dependence 0111 adiance and extrapolate to convert to the radiance values observed in the fire spectra. We apply this extrapolated gain to the spectra in the frequency range near 1000 cm^{-1} (10 μm) where signal levels for the fire views and the 350 K blackbody are comparable. 1 lowever. this extrapolation is not reasonable for the 2000 cm^{-1} (5 μm) region shown in 1 ig. 3 where the fire and the 350 K blackbody signal levels differ by over an order of magnitude and gain dependence on radiance is indeterminate. Although uncalibrated spectra will retain a flux contribution from the instrument radiance that is significant for the view of the unburned area, it contributes less than 10% of the signal level in the fire observation.

The field of view (FOV) in these observations is 3."/5 by 1.94 mrad giving a ground footprint of 45 m by 23 m from 12 km altitude. The footprint is therefore likely to be inhomogeneous, *i.e.* a variety of areas with different surface radiance values, especially in views where the flames were targeted but did not fill the FOV. Fig. 4 shows a likely scenario for the AES FOV during fire data acquisition based on the (visible) video recorded during the tracking sequence.

Spectral Modeling and Analysis

in order to quantify the species detected in the fire spectra wc have dewc.loped three types of physical models for the ground radiance and atmospheric radiative transfer based on the viewing scenario shown in Fig. 4. The models will be referred to as:

1. Smoke plume over unburned ground
II. Embers
111. l'lames.

For each type of model, the ground temperature and the temperature and abundance profiles for atmospheric gases at prescribed altitudes are specified and a simulated spectrum is generated by solving the equation of radiative transfer [e.g., *Goody and Yung,* 1989] using the HITRAN 92 molecular line-by-line database [*Rothman, et al.,* 1992]. The code used for generating spectra from these models is called SEASCRAPE: Sequential Evaluation Algorithm for Simultaneous and Concurrent Retrieval of Atmospheric Parameter Estimates [*Sparks et al.,* 1991].

Table 1. Model layers and parameters for simulated spectra

	I. Smoke over unburned ground weight = 46% OR fire FOV weight = 60% CA fire FOV	II. Embers weight = 49% OR fire FOV weight = 34% CA fire FOV	III. Flames weight = 5% OR fire FOV weight = 6% CA fire FOV
1 km	T = 305 K H_2O, CO_2, CO, N_2O, CH_4, O_3, NH_3, OCS	T = 305 K H_2O, CO_2, (X), N_2O, CH_4, O_3, NH_3, OCS	T = 325 K H_2O, CO_2, CO, N_2O, CH_4, O_3, NH_3, OCS
500111		T_{smoke} = 330 K H_2O, CO_2, (X), N_2O, CH_4, O_3, NH_3, OCS HCOOH, CH_3OH	T_{smoke} = 375 K H_2O, CO_2, CO, N_2O, CH_4, O_3
100 m	T smoke = 350 K H_2O, CO_2, CO, N_2O, CH_4, O_3		T_{smoke} = 450 K H_2O, CO_2, CO
32 m			$T_{transition}$
30 m			T_{flames}
20 m		T_{smoke} = 400 K H_2O, CO_2, CO, NH_3, HCOOH, CH_3OH	H_2O, CO_2, CO
0 m	T_{ground} = 310 K	T_{ground} = 500 K	T_{ground} = 500 K

Table 1 shows the layers and specified parameters for the three models below 1 km, The three types of models all have-the same specifications for 1 km [o 1?. km and use assimilated temperature and height profiles for these dates and locations, provided by the NMC [*Gelman,* 1994]. We assume a relative humidity of 35% at 1.5 km for the Oregon fire location and 20% at 1.5 km for the California fire location. Above 1 km, we assume abundance levels for CO_2 (357 ppm), CH_4 (1780 ppb) and N_2O (312 ppb) based on projecting 1993 values [*Dlugokencky et al.,* 1994; *Halpert et al.,* 1993]. Methane is

included in the models, but does not produce any significant spectral features in the frequency ranges used for this analysis. The CO abundance in the models decreases linearly from 150 ppb at 1 km to 75 ppb at 1.5 km. Although CO does not have very predictable abundance levels, this appears to be a reasonable assumption based on measurements by *Harriss et al.*, [1994].

Because of the inhomogeneity of the scene in our FOV, we have no way of uniquely determining the ground temperatures in our models from our spectral radiance. We must therefore set these temperatures to reasonable values. We use 500 K for the embers and flames models, based on other fire radiance measurements [*Kaufman et al., 1992*], and we use 310 K for the unburned ground based on the average brightness temperature of spectra taken away from the fire areas.

The three models are combined with weights that allow a reasonable match to the observed radiance levels in the spectra from 950 to 1150 cm^{-1}. (The weights must add to 100% and are shown in Table 1). Fig. 5 shows the match of the weighted model combination to the Oregon fire data as well as the individual model components. The combined model spectrum is then scaled (or "decalibrated") to match the spectral data in the 1960 to 2060 cm^{-1} region. At this point, individual parameters in the models, such as flame temperature or single species abundance can be varied for a best fit to the spectral features in the data. Unfortunately, the species with the largest fire emissions, H_2O and CO_2, have a large normal atmospheric abundance and therefore too many model parameters to be varied manually. Quantization of the abundance parameters for these species would require a more sophisticated retrieval technique capable of iterating and optimizing parameters for the three models simultaneously. Although it was not possible to determine uniquely the excess H_2O and CO_2 from the fires in this analysis, our data are consistent with large excess abundances since models with normal atmospheric abundances for these species were clearly inadequate. The H_2O and CO_2 abundance parameters in the models are set to values that give a close enough match to the data so that the estimation of other quantities is not impeded.

No large enhancement in the O_3 abundance was observed and a reasonable fit to the data is obtained with a uniform O_3 abundance at 60 ppb. We do not expect to observe a significantly increased O_3 abundance since O is not produced directly by the fire [*Hegg et al.*, 1990] and our measurements do not include the down-stream fire plume. We also observe CFC-12 (CF_2Cl_2) and OCS and we use these to fit the spectral features for these molecules with an abundance of CFC-12 around 400 ppt and an abundance of OCS around 1 ppb. CFC-12 has been detected in biomass fire emissions [*Hegg, et al.*, 1990], most probably from pollution deposited over time and resuspended by the fire. However, at these low levels, we are not sensitive to an excess abundance in these species over their normal atmospheric abundance.

Flame Temperature:

The flame temperatures in the observed fires are determined by varying the temperature and CO abundance in the flames region (0 to 30 m) of the flames model and comparing the resulting spectra to the observed CO emission lines in the 1960-2060 cm^{-1} region, (see Fig. 3). None of these CO emission features are observed in normal atmospheric spectra and, indeed, some (high rotational quantum numbers in the 2-1 vibrational transition) require temperatures of at least 900 K to populate the relevant energy levels. The

line widths and heights have. a dependence on column density as WC.]] as temperature and we therefore find a range of values in column density and flame temperature that produce a reasonable fit to the spectra. The spectra from both fires can be fitted with a range in CO column density of 20 ppm to 40 ppm over 30 m. The best fit for the Oregon fire data was obtained with a range in flame temperature of 1050 to 1 ?00 K, while the California fire data required a higher values: 1250 to 1350 K.

NH_3 Abundance:

Ammonia is a well known component of forest fire emissions and biomass burning has been shown to be a significant source of atmospheric NH_3 [e.g., *Hegg et* al., 1988 and 1990, *Griffith et al., 1991* and *Laursen et al.*, 1992]. NH_3 is produced during the smoldering phase of a fire, as opposed to the flaming phase, [*Griffith, et* al., 1 991; *Yokelson, et al.,* 1995] and dissociates at flame temperatures [*Hampel and Hawley,* 1973]. We therefore expect the highest NH_3 concentrations in the embers component of our observations.

Assuming that the mixture of the three models suffices to describe our fire observation, it is clear from Fig. 5 that the preponderance of spectral signatures is also due to the embers component. We therefore obtain estimates of column density for species produced in the smoldering phase by adjusting the thermal contrast and species abundances in the embers model to produce the best fit to the absorption features. Ammonia absorption features are especially useful in determining the appropriate thermal contrast in this model since the NH_3 transitions have a similar temperature dependence and some of the strong lines saturate at fairly low abundance, around 50 ppm-m. The ammonia abundance is determined by matching the line strength ratios of nearly saturated to saturated lines while the radiance signature of the stronger saturated lines provides the thermal contrast for the embers model. Fig. 6 shows the fire data compared to model spectra for some of the ammonia absorption features. The presence of the weaker NH_3 lines in the California data indicates a higher ammonia abundance than observed in the Oregon fire.

Table II shows the column densities of NH_3 in the embers model that gave the minimum residuals in the ammonia spectral regions for the model spectra subtracted from the fire spectra. A good fit to the Oregon data was obtained by adjusting only the embers model NH_3 abundance with negligible amounts in the **other** models. However, the California data required around 100 ppm-m NH_3 in models I and III in order to obtain a reasonable match. This affected the uncertainty in the embers (model II) amount for the California fire which is reflected in the NH_3 column density error.

CO ***Abundance:***

CO is emitted during both the flaming and smoldering phases of a fire, but predominantly in the smoldering phase [*Griffith, et al* , 1991; *Yokelson, et al.*, 1995]. We quantify the CO abundance from smoldering processes by using CO absorption lines that have a model signature dominated by the embers model (as opposed **to** the emission lines which can only be modeled with the flames model). In Fig. 7 we can see that the CO absorption lines are different for the California and Oregon fires. The broader line widths in the California fire data indicate a higher level of saturation. Both fires have significantly wider absorption lines than observed in spectra taken away **from the** fire area or the embers model spectrum with a background (normal atmospheric) CO abundance. The CO abundances in the first kilometer of the embers model were adjusted to match the absorption line widths and the

resulting column densities are shown in Table II. The first error in the CO column densities corresponds to the statistical uncertainty in fitting the lines, *i.e.*, the changes in abundance that produced no visible change to the model spectrum. The second error is the systematic uncertainty from the background subtraction, where we assumed that the background CO abundance could vary by as much as 50% from our nominal values. This uncertainty is for the entire background column of CO (from ground to airplane), since, unlike the other species in Table II, the background CO column has a significant spectral signature. For comparison with the CO values in Table II, the column density for a background level of 150 ppb CO, 0 to 1 km, would be 0.15 g/m^2 in the embers model.

our model assumes the standard isotopic abundances: 98.654 % $^{12}C^{16}O$ and 1.108% $^{13}C^{16}O$ [*De Bievre, et al.*, 1984], and we were able to fit to the ^{13}CO lines with the model spectrum using the same CO abundance that produced a good model match to the ^{12}CO absorption lines. The ^{13}CO lines were almost undetectable in the embers model with a background CO abundance.

Table 11. Estimated column densities for the Oregon and California wildfires

Species	Frequency (cm^{-1})	column density (molecules/cm^2) OR fire 3/8/94	column density (molecules/cm^2) CA fire 3/15/94	column density (gm/m^2) OR fire 3/8/94	column density (gm/m^2) CA fire 3/15/94
CO (background subtracted)	2050-2135	3.43e+18 (j()," /8,1(1.9"/)('+"18	1.85e+19 (±0.28 ±0.11)e+19	1.59 ± 0.36 ± 0.45	8.60 ± 1.29 ± 0.50
NH_3	960-1160	(1.46 ±(1,1 (1)(',-1-1"	("/.'/'/ ±1.55)e+17	0.041 ± 0.005	0.220 ± 0.044
CH_3OH	1033	(1.56 ±0.20)e+17	(2.95 ± 0.46)e+17	0.083 ± 0.011	0.157 ± 0.024
HCOOH	1105	(8.60 ± 1.50)e+16	(1.12 ± 0.19)e+17	0.066 ± 0.011	0.086 ± 0.015
C_2H_4	949.5	detected	detected		

Methanol, formic acid and ethylene:

Oxygenated organic compounds such as methanol, formic acid, formaldehyde and acetic acid have been previously measured in biomass fire emissions during broadcast burn and laboratory studies [*Griffith, et al.*, 1991; *McKenzie, et al.*, 1994; *Yokelson, et al.*, 1995]. Nonmethane hydrocarbons (NMHC) detected in airborne plume sampling of biomass fires are quantified in *Hegg et al.*, [1990] and *Lamsen, et al.*, [1992], although ethylene is not among the species listed. Ethylene and other NMHCs are measured in *Yokelson, et al.*, [1995]. (Formaldehyde, acetic acid and most NMHCs have their spectral signatures outside the ranges covered in our data set.) *Yokelson, et al.*, [1995], show that these species are due primarily to pyrolysis and distillation rather than smoldering or flaming combustion. We do not have enough independent spectral information to distinguish this type of production from smoldering combustion since it also occurs at high temperature and the produced species combust in the flames. We therefore rely on our "embers" model for quantification of these species and acknowledge that the assumed thermal contrast in this model could be different for the pyrolysis processes. If our assured thermal contrast is too high, then our species abundances will be underestimated.

To estimate the methanol (CH_3OH) and formic acid (HCOOH) column densities in our data, we apply absorption cross-section data from *Hanst and Hanst*, [1993], to our radiative transfer model. Methanol has a peak in absorbance at 1033 cm^{-1} which is somewhat obscured by the O_3 band from 1010 to 1070. The spectral signature in the data is therefore more easily seen after subtracting a model spectrum with a reasonable match to the O_3 lines. Fig. 8 shows the data from the Oregon and California fires after subtracting model spectra generated with no abundance of methanol or formic acid. The model signatures for the best fits to these residuals are overplotted and the column densities of CH_3OH and HCOOH are shown in Table II

Quantifying the ethylene abundance is more problematic. The peak absorbance at 949.5 cm^{-1} coincides with a CO_2 line and is also on the edge of the. optical filter passband, which results in poor radiometric calibration and SNR at frequencies below 950 cm^{-1}. We observe ethylene by noting excess absorption at the 949.5 cm^{-1} CO_2 line compared to the other nearby CO_2 absorption lines which appear thinner and are reasonably matched by the model spectrum. The depth and width of this excess absorption in the Oregon fire data can be fitted using a model spectrum with an ethylene component CU7114 column density around 1.0e+17 molecules/cm^2. However, this estimate has very large errors due to the unquantifiable uncertainties in (l.)? abundance as well as the poor calibration and SNR.

Comparisons to other measurements:

Since our data are taken over the hottest regions of these fires, we expect our measurements to be somewhat different from aircraft plume sampling, for example, where gases emitted by the fire are probably sampled after they have moved away from their sources. The more relevant comparisons for our results are with ground based remote sensing data where measurements are made of fire. emissions from their flaming or smoldering sources. Many results are presented in quantities of emission factors (mol/kg fuel) or emission ratios relative to CO_2. Since we are unable to calculate these quantities from our results, we compare emission ratios relative to CO with other measurements converted to this emission ratio.

For NH_3/(X) (mol/mol) we measure 0.043 ± 0.016 (OR fire) and 0.042 ± 0.011 (CA fire) in what we assume is smoldering emission. *Yokelson, et al.*, [1995], using a variety of fuels mixtures in a laboratory combustion chamber, report values giving a range in NH_3/CO ratio of 0.009 to 0.034 (taken from all the measurements, using the smoldering combustion only for fires with results quoted for the different fire. phases). Lower ratios were found for fuel compositions of only pine needles or sage.brush and higher ratios for more heterogeneous fuel mixtures of duff twigs, pine needles and wood. Field measurements from four broadcast fires in *Griffith, et al.*, [1991] give a ratios of 0.008, 0.017, 0.046 and 0.059 for NH_3/CO with the higher ratios for brush and grass fires compared to logging waste burns. *Hegg et al.* [1988] report a range of 0.002 to 0.038 with an average of 0.012 ± 0.005 for NH_3/CO from aircraft smoke plume sampling. Our best agreement is with the *Griffith, et al.*, [1991] results for brush and grass fires which we believe to be more similar to the fires we observed than the fires studied by *Yokelson, et al.*, [1995]. It also seems reasonable to expect different results for the smoke plume ratio compared to the emission ratio directly over smoldering areas.

For methanol, we calculate CH_3OH/CO emission ratios of 0.016 and 0.046 (mol/mol). The results from *Yokelson, et al.*, [1995] give a range of 0.005 to 0.031, again, with larger

ratios from the fires with heterogeneous fuel mixtures. *McKenzie, et al., [1994]* report a molar ratio of 0.025 for methanol to CO from smoldering combustion of ponderosa pine sapwood.

Our formic acid to CO molar ratios are 0.006 and 0,0?5. in the fires studied in *Yokelson, et* al., [1995], HCOOH was below the detection limit in all but one: the fire set to simulate a "crown" forest fire by using a fuel mixture of green pine needles and twigs Over dry needles and wood. The results 1 rom this "crown" fire give the ratio 0.007 for HCOOI I/CO. For smoldering combustion of ponderosa pine **sapwood,** *McKenzie, et al., [1994]* report a molar ratio of 0.004 for formic acid 10 CO.

Given the large ranges in values for different fires and fuel types, our emission ratios are comparable with previous measurements. We confirm the results of *Griffith, et al., [1991], McKenzie, et al., [1994]* and *Yokelson, et al.*, [1995] showing a significant presence of methanol and formic acid in biomass burning emissions. Sources of atmospheric concentrations of these species should receive more attention since oxygenated hydrocarbons such as methanol have recently been shown to play an important role in tropospheric photochemistry [*Singh, et al*, 1995].

Unmatched Emission Features:

Although we are fairly certain that we have identified the obvious absorption features in our data, there are emission features that we are unable to match using our three. component model with the 1992 HITRAN database [*Rothman, et al.*, 1992], as illustrated in the upper panel **of** Fig. 9. Based on **the** features that are modeled, **the.** strong emission lines in our data are from transitions occurring at high temperatures, *i.e.* in the flames of the fire. This precludes many species from consideration and after comparing sunspot spectra in the same frequency ranges [*Wallace, et al.*, 1992, 1994, 1995], we conclude that the primary candidates for these emission lines are hot H_2O and CO. A few emission lines in the data also matched known high excitation transitions **of** CO_2. **It** is not surprising **that we** do **not** match all the emission features using the HITRAN92 linelist since the database was intended for terrestrial atmospheric studies at normal temperatures (around 300 K). This results in known defects for H_2O when the database is applied at high temperatures [*Schryber, et al.*, 1995]. A preliminary investigation **indicates that** many of the emission features in our data can be modeled by extending the spectroscopic database to include high temperature transitions of H_2O, CO and possibly CO_2. The bottom panel of Fig. 9 shows a calculation with high excitation lines of H_2O at 2048.33 cm^{-1} and CO at 2051.076 cm^{-1} in addition to the HITRAN92 linelist The identifications are based on assignments given in the solar atlas of *Wallace and Livingston*, [1992] and the parameters in the HITEMP high temperature molecular database. [*Rothman, et al., 1995].* The features were simulated without modification of the HITRAN parameters except for a shift in the position of the H_2O line. by -0.05 cm^{-1} to agree with the position reported in the solar atlas.

Conclusions

As a proof of concept, we have shown the utility of the airborne spectral remote sensing technique in measurements of emissions from biomass fires. Although we did not have a sophisticated retrieval method for this data analysis, it is obvious that there were large amounts of water vapor, carbon dioxide, carbon monoxide, ammonia, methanol, formic

acid and ethylene emitted by the fires we observed. Increased understanding of the impact of biomass burning emissions, including oxygenated organics, to atmospheric chemistry requires better and more comprehensive quantification of the emitted species. Since many reactive species are difficult to measure with *in situ* sampling but, in principle, pose no problem for spectral remote sensing, this technique could provide a useful complement to the plume sampling methods normally used for fire measurements.

Our temperature and species abundance retrievals could be dramatically improved with planned experiments over instrumented broadcast burn sites that provide "ground truth" data to verify our physical models. Some commonly emitted species such as methane or formaldehyde were simply outside the spectral range in these observations and would require only minor modifications for detection. We further note that the performance of AES has improved considerably since these data were acquired and new fire measurements would have reduced uncertainties.

Acknowledgments

The authors would like to thank Thomas A. Glavich, Ronald G. Holm, Steven A. Larson, Jack S. Margolis, Sumita Nandi, Wallace M. Porter, David M. Rider, Lawrence C. Sparks and Ronald E. Steinkraus without whose dedicated efforts these measurements could not have been made.

The research described in this paper was conducted by the Jet Propulsion Laboratory, California Institute of Technology under a contract with the National Aeronautics and Space Administration.

References

Bureau of Land Management, Moro, Oregon, private communication, January, 1995

California Dept. Forestry and Los Padres Forest Service, San Luis Obispo, California, private communication, January, 1995

Crutzen P.J. and M.O. Andreae, "Biomass burning in the tropics: impact on atmospheric chemistry and biogeochemical cycles", *Science* **250**, 1669-1678, 1990.

De Bievre, P., M. Gallet, N. E.) Holden, and I 1. L. Barnes, "Isotopic abundances and atomic weights of the elements", *J. Phys. Chem Ref. Data* **13**, 809-891, 1984.

Dlugokencky, E.J., 1..1-'. Steele, P.M. Lang and K.A. Masatie, "The growth rate and distribution of atmospheric methane", *J. Geophys. Res.* 99, 1 '/021 - I 7043, 1994.

Gelman, M., National Meteorological Center, private communication, September, 1994.

Goody, R.M. and Y. L. Yung, *Atmospheric Radiation Theoretical Basis*, 2nct Edition, 1989, Oxford University Press, New York, Oxford. (The equation of radiative transfer is described in this and numerous other texts).

Griffith, D. W.T., W.G. Mankin, M T Coffey 1 D.E. Ward and A. Riebau, "FTIR remote sensing of biomass buring emissions of ('O2, CO, CH4, CH2O, NO, NO2, NH3 and N2O", Levine, J.S. ed.: *Global Biomass Burning: Atmospheric, Climatic and Biospheric Implications, 1991,* Cambridge: MIT Press.

Halpert, M. S., G.D. Bell, V. E. Kousky and C. F. Ropelewski, editors: *5th Annual Climate Assessment, 1993,* NC) AA, U.S. Department of Commerce.

Hampel, C.A. and G.G. Hawley, editors *Encyclopedia of Chemistry, 3rd* Edition, p. *71, 1973,* Van Nostrand Reinhold, New York

Hanst, P.L. and S.'J'. Hanst, data base and atlas *Infrared Spectra for Quantitative Analysis of Gases*, 1993, Infrared Analysis, Inc., 1:34 N. Knollwood Circle, Anaheim, CA, 92801.

Harriss, R, C., *et* al., "Carbon monoxide and methane over Canada: July-August 1990", *J. Geophys. Res. 99,* 1659-166°, 1994,

Hegg, D. A., L.F. Radke, P.V. Hobbs, and P.J. Riggan, "Ammonia emissions from biomass burning", *Geophys. Res. Letts.* **15**, 335-337, 1988.

Hegg, D. A., L.F. Radke, P.V. Hobbs, R. A. Rasmussen and P.J. Riggan, "Emissions of some trace gases from biomass fires", *J. Geophys. Res.* 95, 5669-5675, 1990.

Kaufman, Y. J., A. Setzer, D. Ward, D. Tanre, B.N. Holben, P. Menzel, M.C. Pereira and R. Rasmussen, "Biomass Burning Airborne and Spaceborne Experiment in the Amazonas (BASE-A)", *J. Geophys. Res.* 97, 1'15:11-14 599, 199?.

Laursen, K. K., P.V. Hobbs, L.F. Radke and R.A. Rasmussen, "Some trace gas emissions from North American biomass fires with an assessment of regional and global fluxes from biomass burning", *J. Geophys. Res.* 97, ~'(Kh/-20"/01, 1992.

McKenzie, L.M., W.M. Hao, G.N. Richards and D.E. Ward, "Quantification of major components emitted from smoldering combustion of wood", *Atmos. Environ.* 28, 3285-3292, 1994.

Rothman, 1.. S., R.R. Gamache, R.H. Tipping, C.P. Rinsland, M.A.H. Smith, D.C. Benner, V.M. Devi, J.-M. Flaud, C. Camy-Peyret, A. Perrin, A. Goldman, S.'1'. Massie, L.R. Brown, and R.A. Toth, "The HITRAN molecular database: editions of 1991 and 1992", *J. Quant. Spectrosc. Radiat. Transfer 48,169507,* 1992.

Rothman, 1,. S., R.B. Wattson, R.R. Gamache J. Schroeder and A. McCann, "HITRAN HAWKS and HITEMP high-temperature molecular database, *SPIE,* 2471, in press, 1995.

Schryber, J.H., S. Miller and J. Tennyson, "Computed Infrared Absorption Properties of 1 lot Water Vapour", *J. Quant. Spectrosc. Radiat. Transfer* **53**, 373-380, 1995.

Singh, }1.13., M. Kanakidou, P.J. Crutzen I, D. Jacob, "High concentrations and photochemical fate of oxygenated hydrocarbons in the global troposphere", *Nature* 378, 50-54, 1995.

Sparks, 1... P. Lyster, J.E. Patterson and J.J, Tanselow, "I ,argc-scale retrieval of atmospheric parameters from remote sounding data", Technical Digest on Optical Remote Sensing of the Atmosphere, 1991 (Optical Society of America, Washington, D. C.) Vol. 18, pp. 75-77, 1991.

Wallace, L. and W. Livingston, " AT I atlas for a dark sunspot umbral spectrum from 1970 to 8640 cm^{-1} (1.16 to 5.1 μm)", National Solar Observatory Technical Report #192-00 1, National Solar Observatory, Tuscon, AZ, 1'**)9,**'

Wallace., L., W. Livingston, and 1'. Bernath. "AT I Atlas of the Sunspot Spectrum from 470 to 1233 cm^{-1} (8.1 to 21 μm) and the photospheric spectum from 460 to 630 cm-l (16 to 22 pm)", National Solar Observatory Technical Report /194-001, National Solar Observatory, Tucson, AZ, 1994.

Wallace, 1.., I'. Bernath, W. 1 Livingston, K Hinkle, J. Busler, B. Guo, K. Zhang, "Water on the Sun", *Science* 268, 11 S5- 1158.1995

Yokelson, R. J., D. .W.T. Griffith and 1 D.I Ward, "Open-path 1 'TIR studies of]argc-scale laboratory biomass fires", submitted to *J. Geophys. Res.*, August, 1 995.

Figure Captions

Fig. 1. optical schematic of the Airborne Emission Spectrometer (AES). (The periscope is rotated 90° for clarity). CCR = cube-corner reflector; 131,2,3 = dichroic beamsplitters; Ml ,2,3,4 = fold mirrors; IA, 2A, 1 B, 2B, detector dewar identifications (with corresponding spectral coverage shown. The interferometer itself is maintained under a low vacuum to protect hygroscopic components and reduce acoustic coupling into the optical path.

Fig. 2. AES spectra from (a) the Oregon fire, (b) the California fire and (c.) an unburned area upwind of the California fire. In all the spectra shown in this paper, the instrument view is downlooking with a maximum off-nadir angle of 30°. The overall shape and radiance.hwc] of the spectrum is dominated by the average ground radiance in the footprint while the sharp features (the spectral "lines") are from molecular transitions in the atmospheric gases along the line of sight. Lines with radiances above the. ground radiance are in emission while lines with radiance values below this level are in absorption. Absorption features due to gases released by the fires are labeled in the fire spectra while the features due to species with significant normal atmospheric abundance are indicated in the spectrum of the unburned area. '11](emission lines in these fire spectra are mostly from hot CO_2 and 1120.

Fig. 3. Uncalibrated AES spectra from (a) the Oregon fire, (b) the California fire and (c) an unburned area upwind of the (lilifolll~:i fire. Although the fluxes in these spectra have not been converted to radiance units, (see text for details), it is possible to compare their spectral features such as the]'JI'OJ"llill('lll emission lines in the fire spectra and the lower signal to noise ratio in the spectrum from the unburned area. The labeled emission lines correspond to the CO transitions used for estimating the flame temperatures.

Fig. 4. Likely scenario for the view contained in the AES footprint during fire data acquisition.

1 'ig. 5. (top) Comparison of the AI ES spectrum from the Oregon fire to a model spectrum made by combining three simulated spectra generated from models of the different fire regimes contained in the AES footprint The model parameters for 0 to 1 km. altitude are shown in table I. (bottom) The spectral contribution from each of the weighted model components. Note that except for emission lines, the "embers" mode] contributes over 75% of the spectral radiance signature but on Is has a weight of 49%.

Fig. 6. Some of the ammonia absorption features present in the fire spectra. (a) Oregon fire data with match to the weighted combination of the three fire model components. (b) California fire data with model match. (c) Simulated ammonia signature. (This spectral region includes the Q-branch, near 965 cm^{-1})

Fig. 7. Comparison of CO absorption lines for the California and Oregon fires. On this vertical scale, the background spectrum, (taken away from the fire region) would have flux levels around 0.04 (see figure ?). 1 Due to the high signal level and larger CO abundance we can also observe the rarer ^{13}CO isotopic transitions.

Fig. 8. Oregon and California fire spectra with model subtraction. The upper plots show the difference between the Oregon fire data and the best model match that does not include CH_3OH or HCOOH. The lower plots show this difference for the California fire data where the fit to the O_3 lines was not as good. Methanol and formic acid signatures are clearly seen as the broad (> 1 cm^{-1} FWHM) absorption features that produce a negative residual. The sharp positive residual features are due to poorly modeled H_2O and unmodeled emission lines. The dotted lines show the model residual: model spectra including CH_3OH and HCOOH minus model spectra with no CH_3OH or HCOOH.

Fig. 9. AES data from the California fire compared to model spectra. This spectral range shows two emission features that we are unable to match using only the molecular transitions in the HITRAN92 database (top plot) and the match to these lines when additional transitions are included in our model (bottom plot). The added transitions in the lower plot are H_2O at 2048.33 (III] with rotational transition (20, 3, 18) to (19, 2, 17) in the 010-000 vibration band and (X} at 2051.076 cl]]"], the P1 O rotational transition in the 3-2 vibration band. Note that the same species abundances are used to create the model spectra in both plots and we obtain a reasonable fit to other H_2O and CO features that are present in this spectral range,.

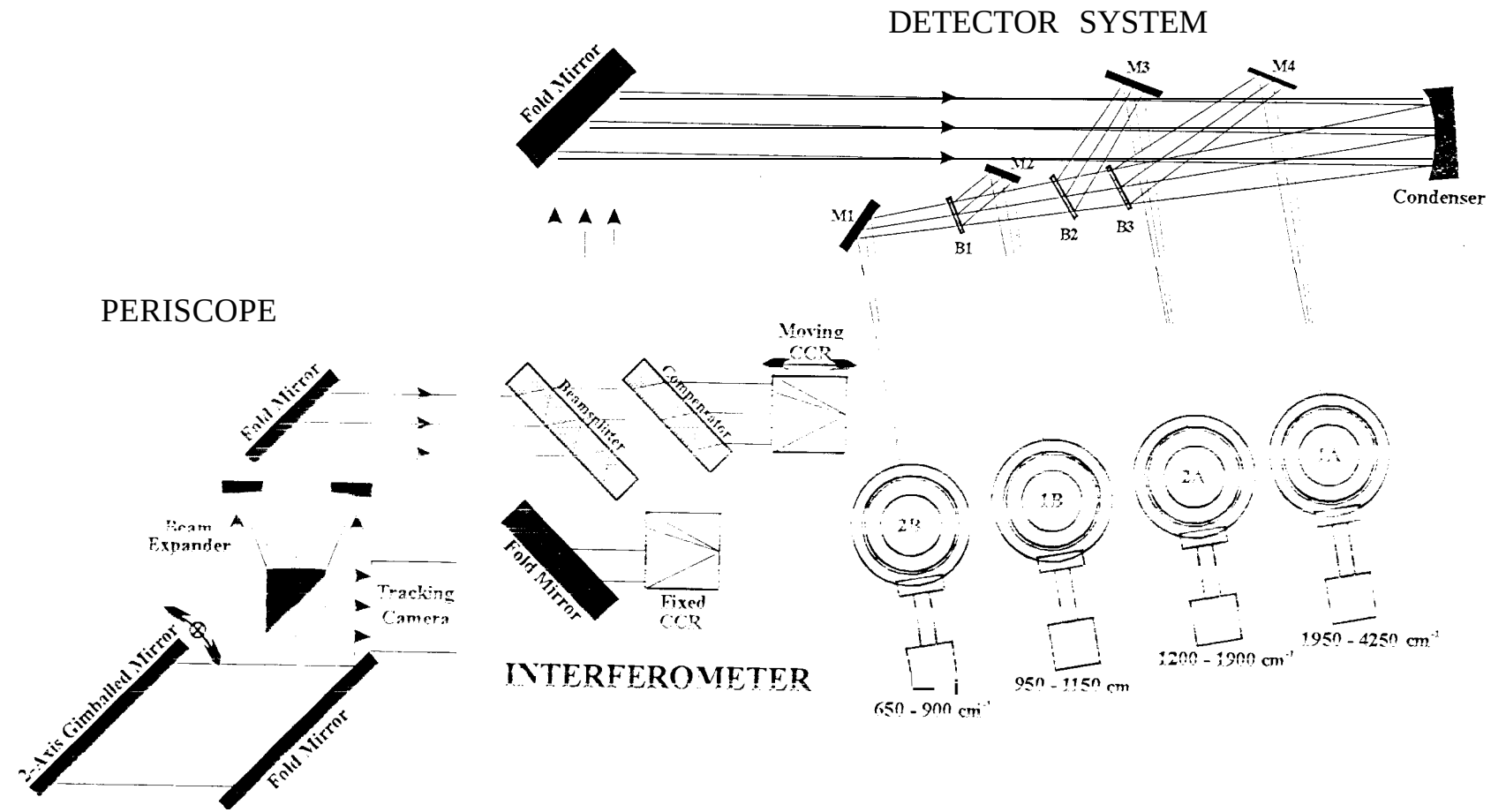
DETECTOR SYSTEM
Fold Mirror
M3
M4
M2
M1
B1
B2
B3
Condenser
PERISCOPE
Moving CCR
Beamsplitter
Compensator
Fold Mirror
Beam Expander
Tracking Camera
Fixed CCR
2-Axis Gimballed Mirror
Fold Mirror
INTERFEROMETER
2B
1B
2A
1A
650 - 900 cm-1
950 - 1150 cm
1200 - 1900 cm-1
1950 - 4250 cm-1
AAA AA
ZnSe Aircraft Window
From Scene

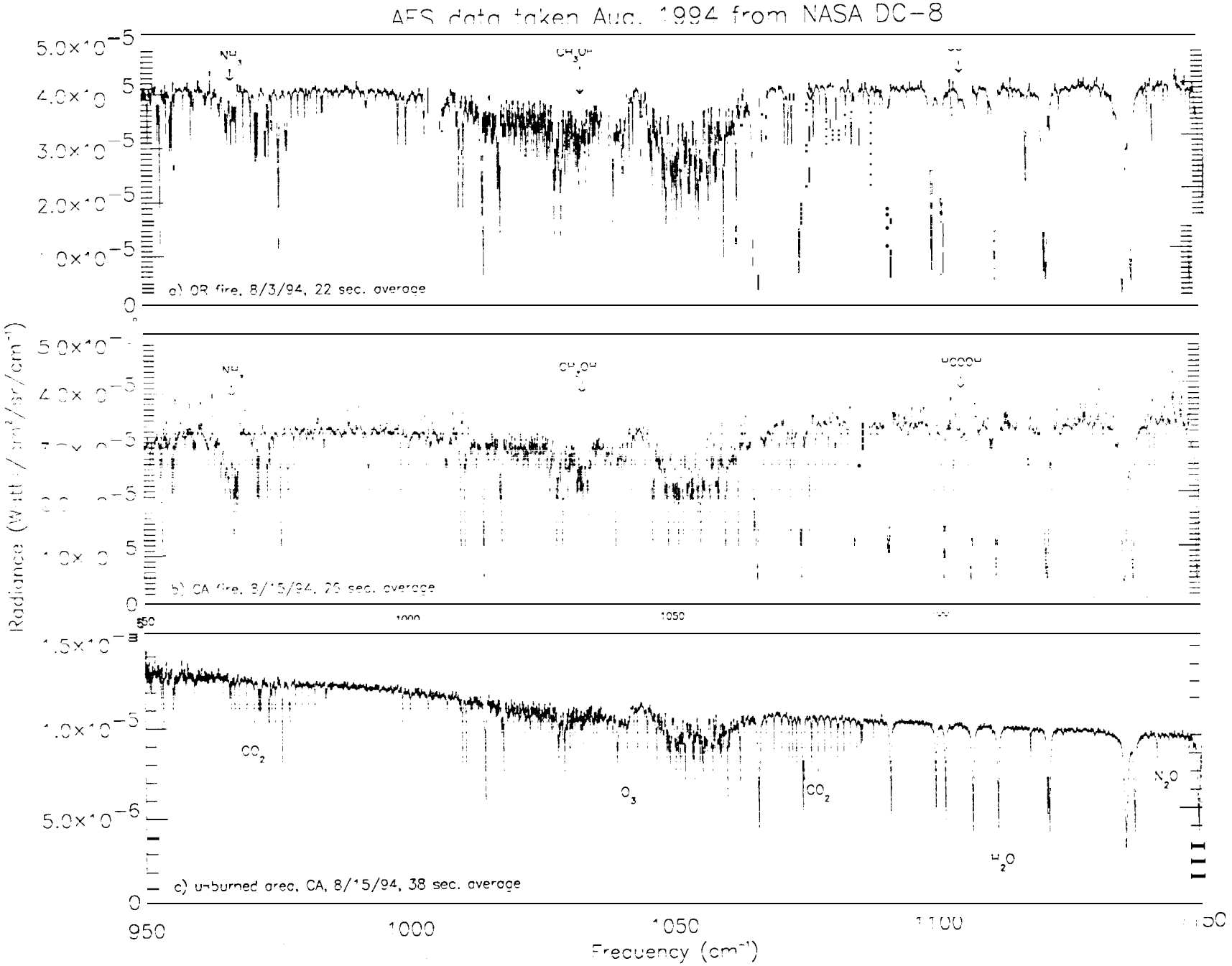
AES data taken Aug. 1994 from NASA DC-8
Radiance (Watt / cm²/sr/cm⁻¹)
a) OR fire, 8/3/94, 22 sec. average
b) CA fire, 8/15/94, 20 sec. average
c) unburned area, CA, 8/15/94, 38 sec. average
CO2
O3
CO2
H2O
N2O
950
1000
1050
1100
Frequency (cm⁻¹)

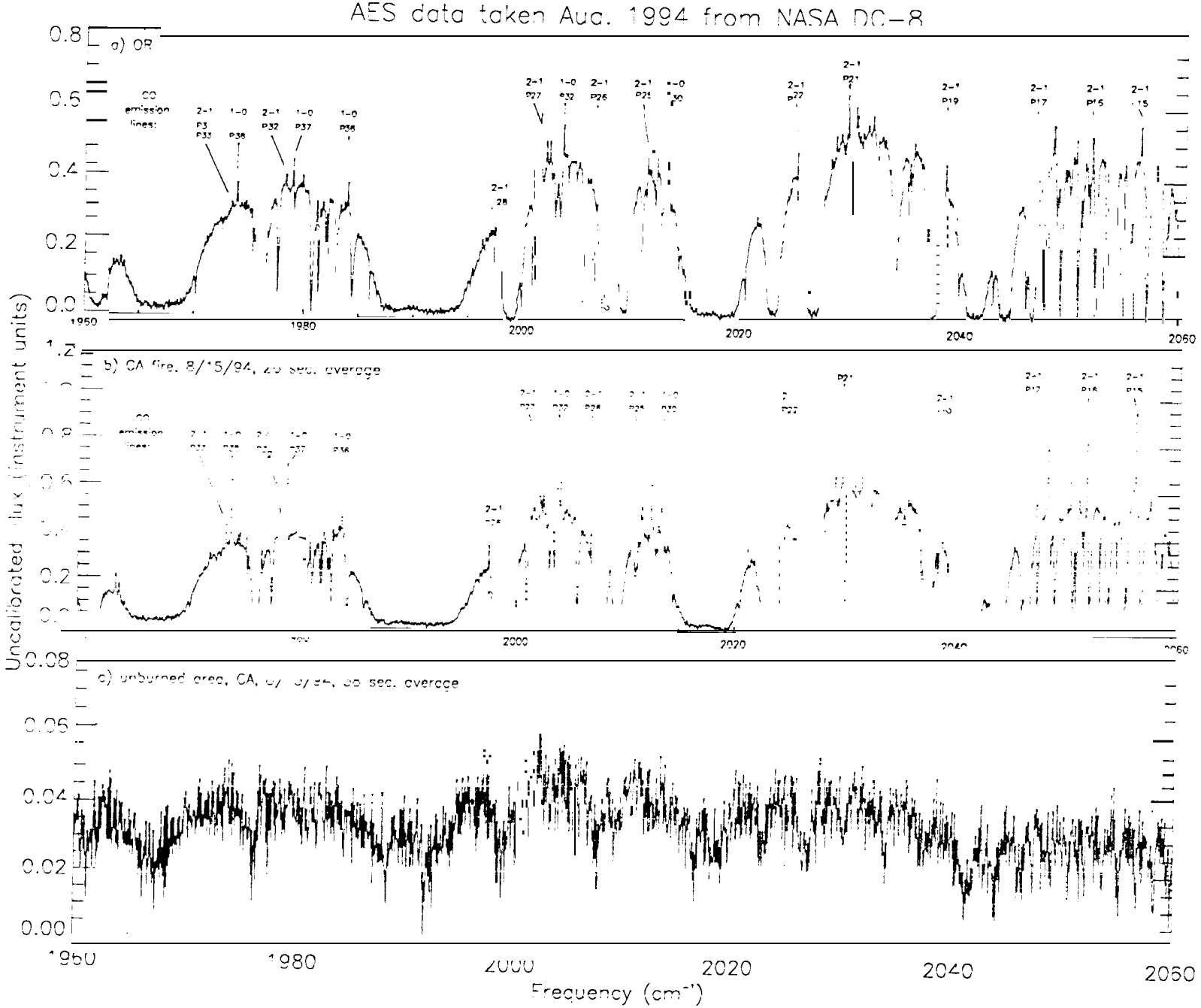
AES data taken Aug. 1994 from NASA DC-8
a) OR
b) CA fire, 8/15/94, 20 sec. average
c) unburned area, CA, 8/ 8/94, 30 sec. average
CO emission lines:
Uncalibrated flux (instrument units)
Frequency (cm⁻¹)
1950
1980
2000
2020
2040
2060

AES Footprint

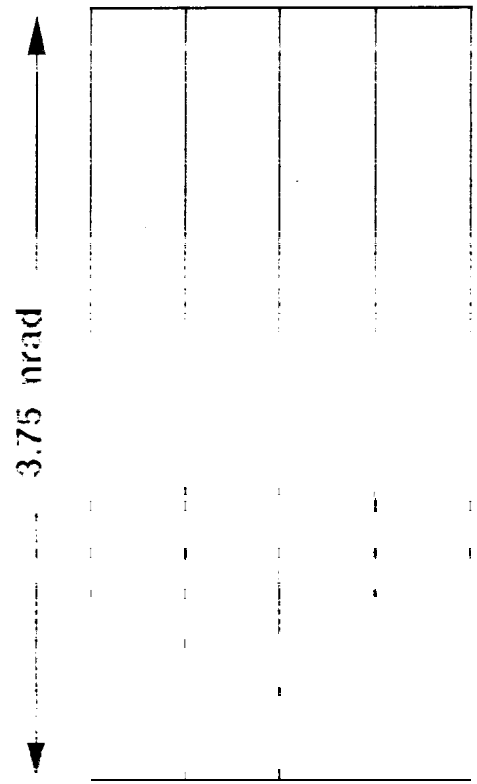

4 pixels

1.94 mrad

(23 mat 39000 ft.)

Fire Scenario

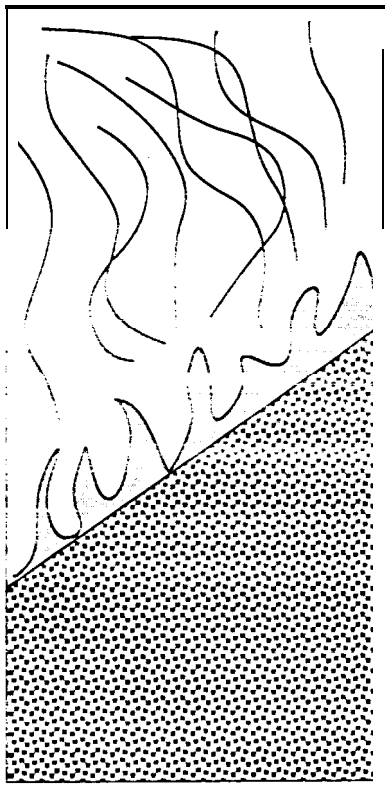

smoke and gas plume over unburned materia

fire line (flames)

smoldering embers (with gas emission)

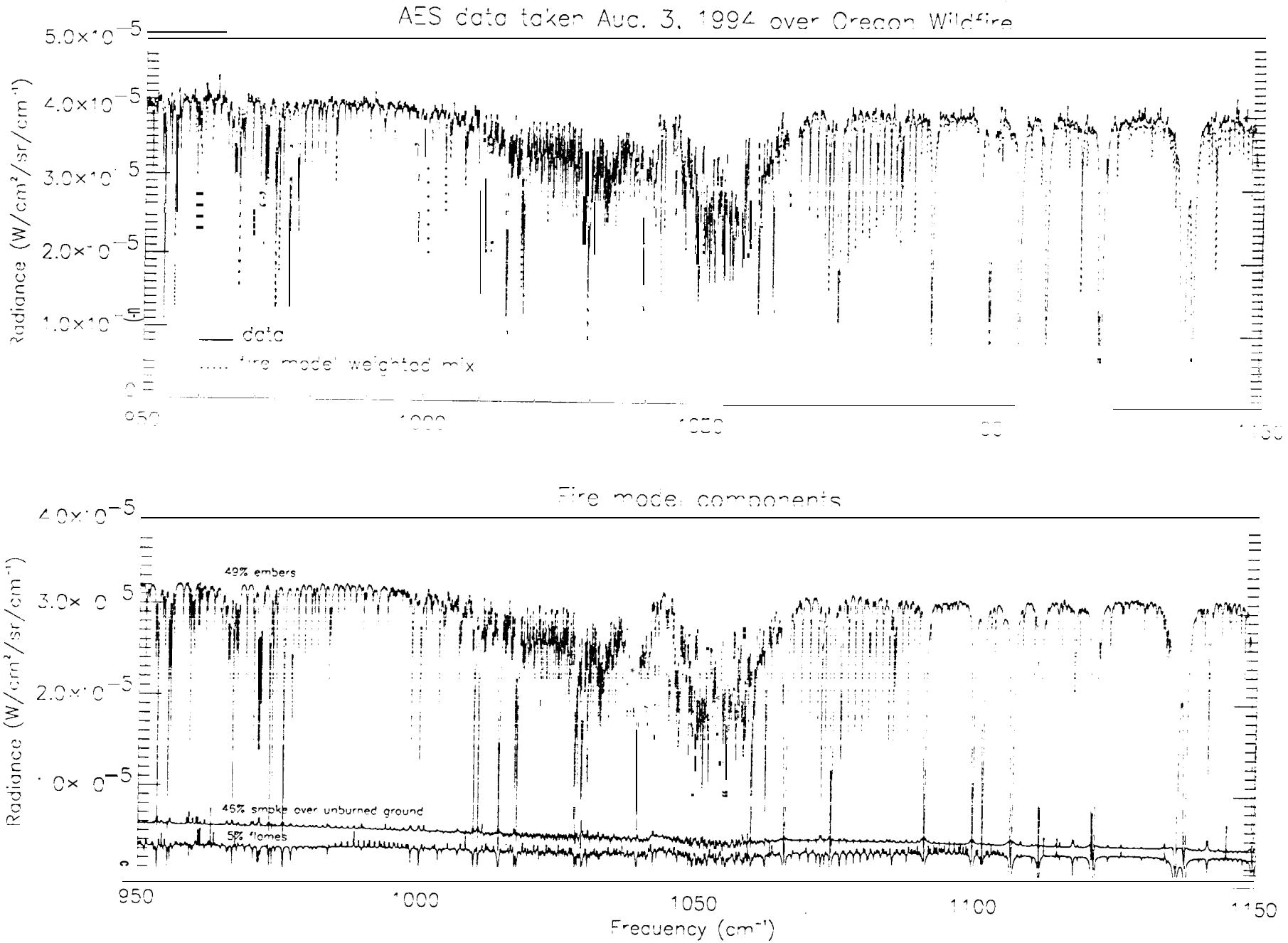
AES data taken Aug. 3, 1994 over Oregon Wildfire
Radiance (W/cm²/sr/cm⁻¹)
data
fire model weighted mix
Fire model components
49% embers
45% smoke over unburned ground
5% flames
950
1000
1050
1100
1150
Frequency (cm⁻¹)

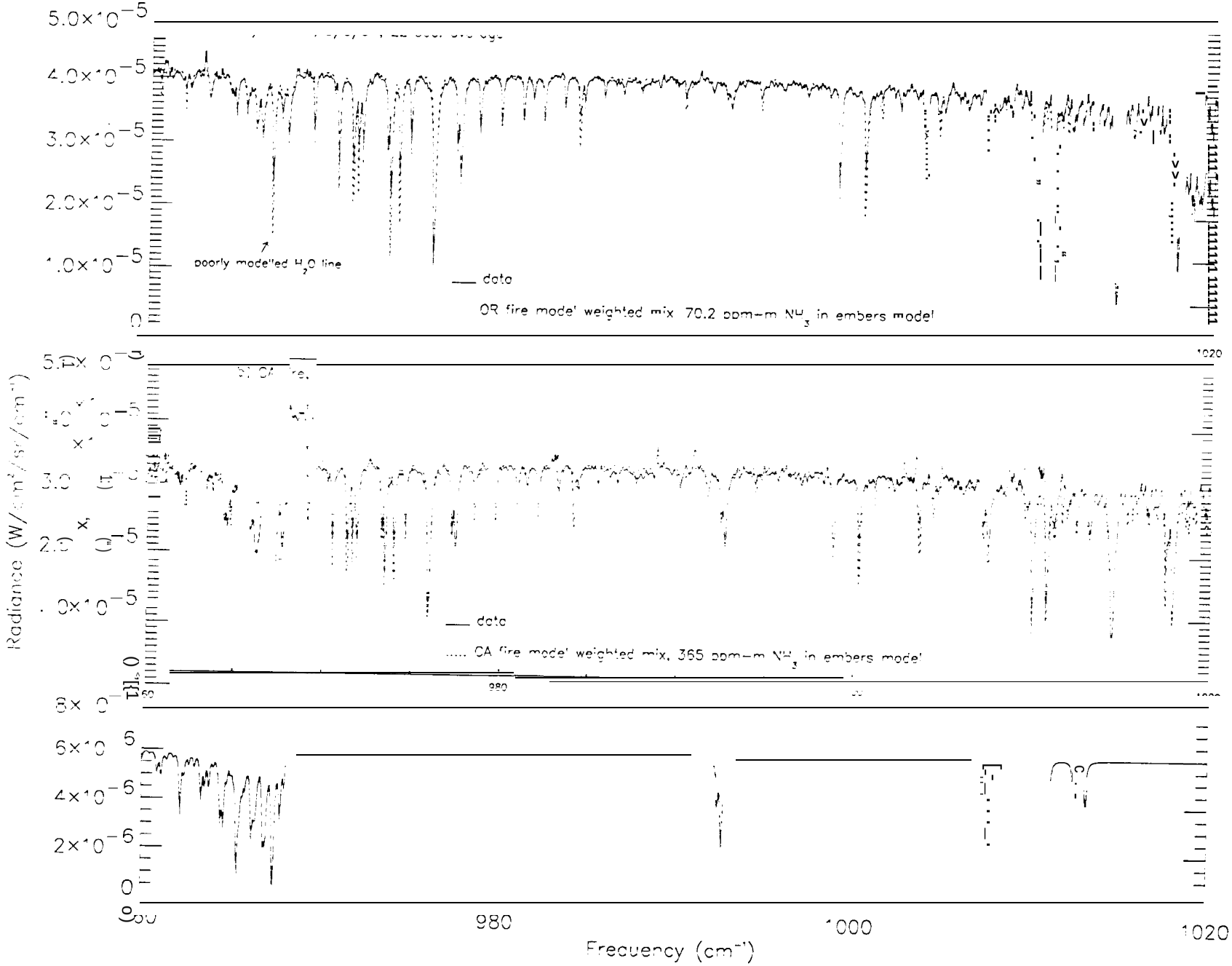
poorly modelled H_2O line
data
OR fire model weighted mix 70.2 ppm-m NH_3 in embers model
data
..... CA fire model weighted mix, 365 ppm-m NH_3 in embers model
Radiance (W/cm²/sr/cm⁻¹)
Frequency (cm⁻¹)
980
1000
1020

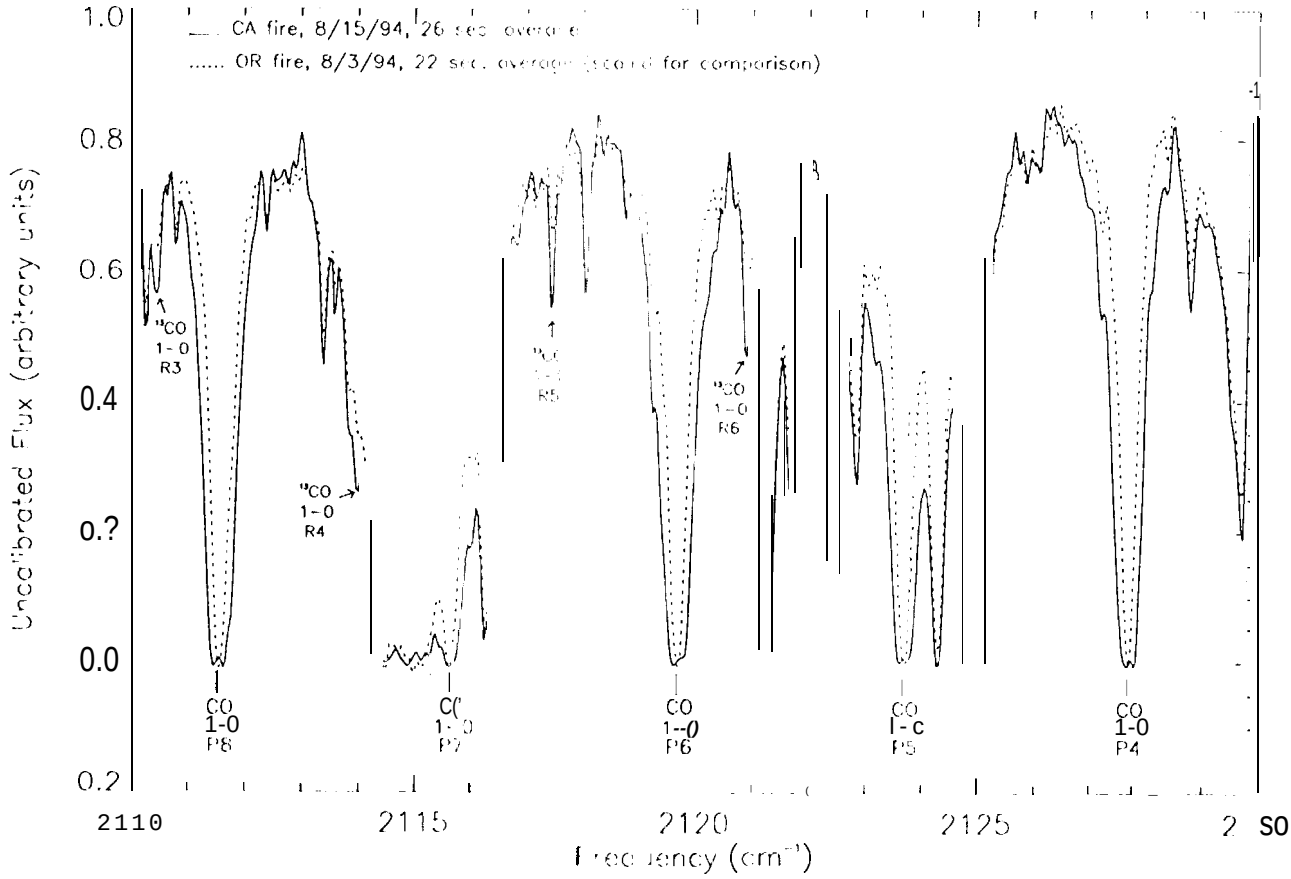
CA fire, 8/15/94, 26 sec. overage
OR fire, 8/3/94, 22 sec. overage (scaled for comparison)
Uncalibrated Flux (arbitrary units)
1.0
0.8
0.6
0.4
0.?
0.0
0.2
13CO 1-0 R3
13CO 1-0 R4
13CO 1-0 R5
13CO 1-0 R6
CO 1-0 P8
CO 1-0 P7
CO 1-0 P6
CO 1-0 P5
CO 1-0 P4
2110
2115
2120
2125
Frequency (cm-1)

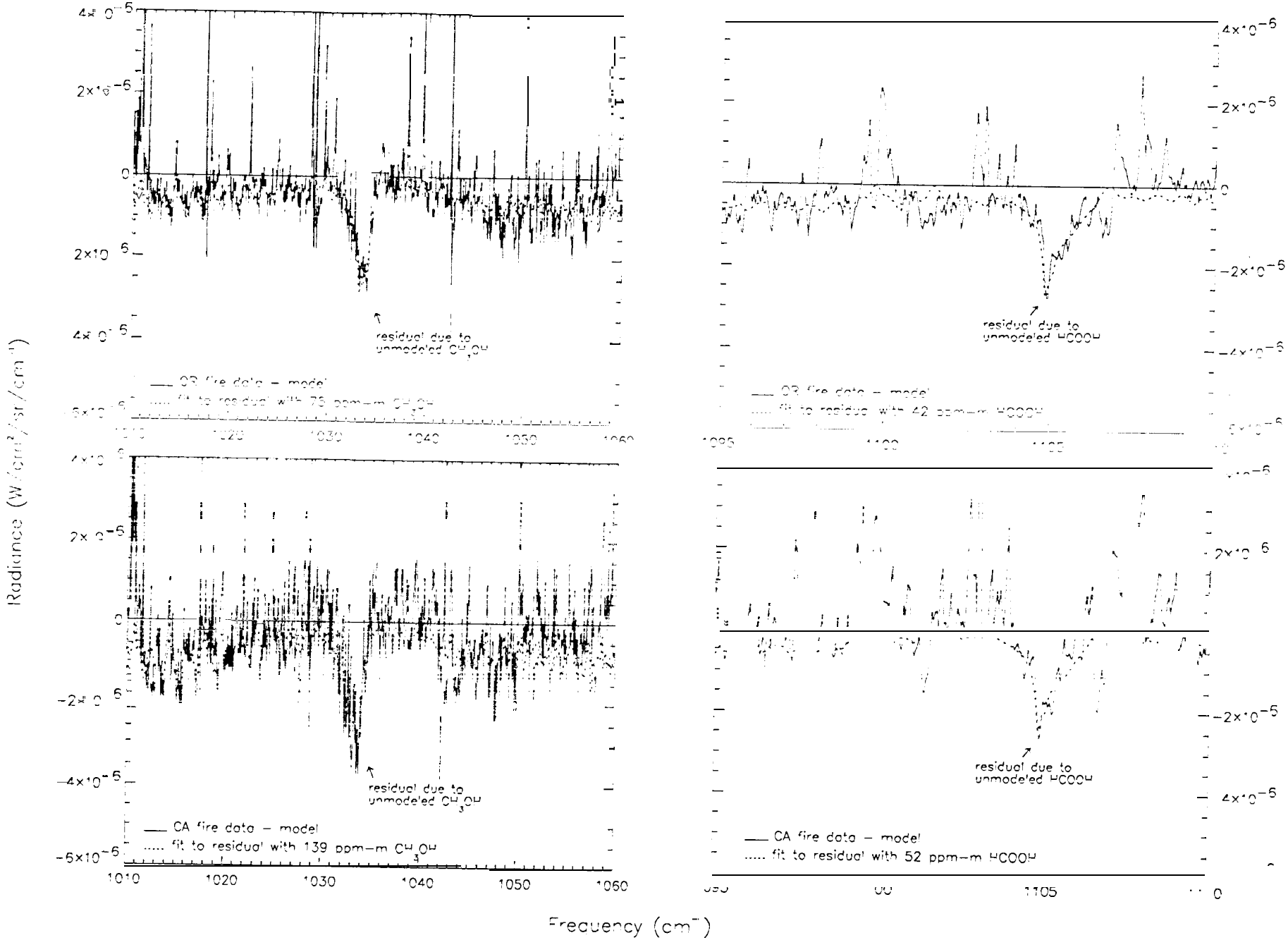
Radiance (W/cm²/sr/cm⁻¹)
residual due to unmodeled CH3OH
CA fire data – model
..... fit to residual with 139 ppm–m CH3OH
residual due to unmodeled HCOOH
CA fire data – model
..... fit to residual with 52 ppm–m HCOOH
Frequency (cm⁻¹)

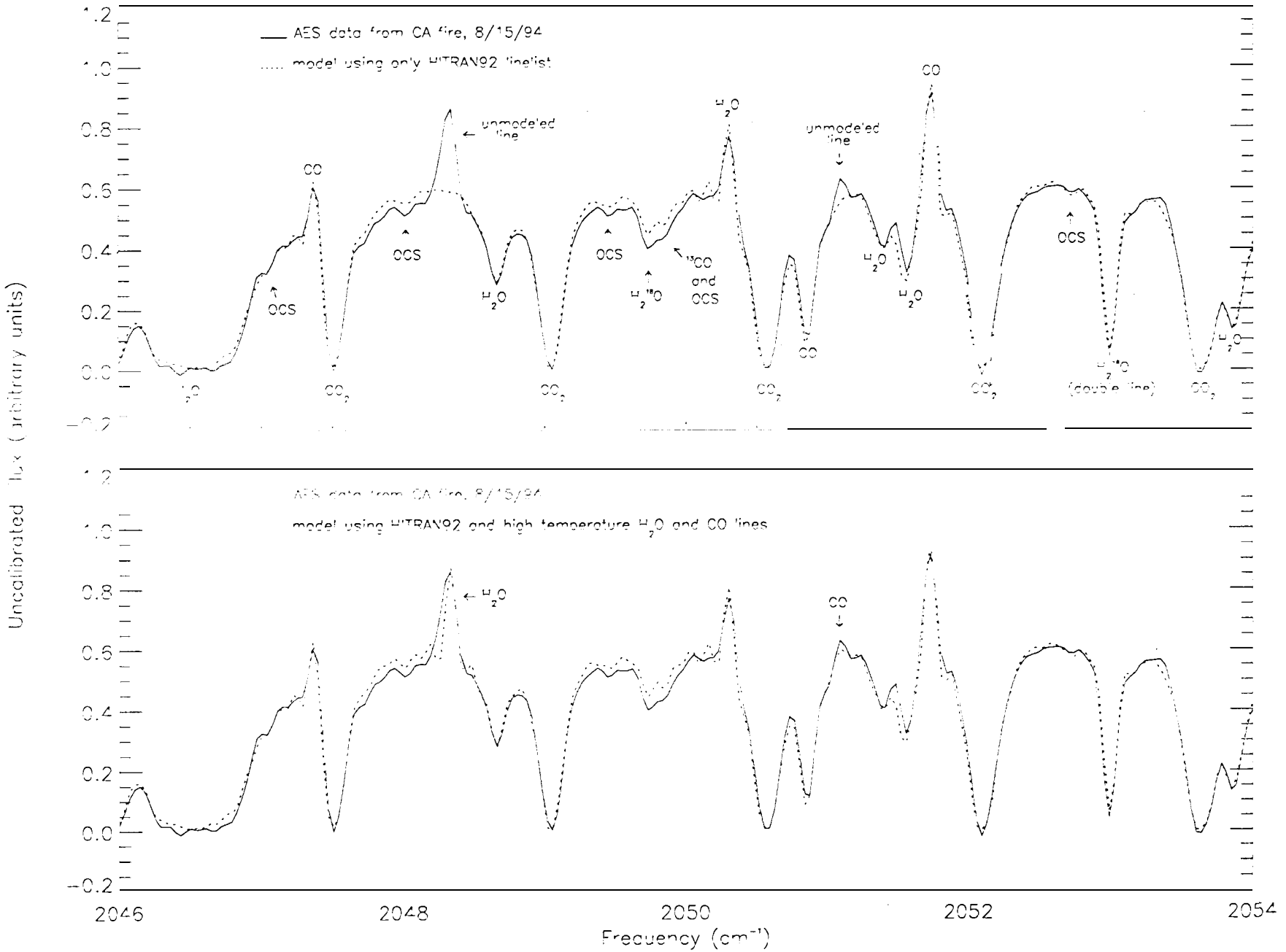
AES data from CA fire, 8/15/94
..... model using only HITRAN92 linelist
unmodeled line
CO
OCS
H_2O
CO_2
$H_2{}^{18}O$
^{13}CO and OCS
CO
AES data from CA fire, 8/15/94
model using HITRAN92 and high temperature H_2O and CO lines
Uncalibrated flux (arbitrary units)
1.2
1.0
0.8
0.6
0.4
0.2
0.0
-0.2
2046
2048
2050
2052
2054
Frequency (cm^{-1})